arXiv:1409.0289v2 [cs.IT] 3 Sep 2014

Scalable Inference for Neuronal Connectivity from Calcium Imaging

Alyson K. Fletcher
Dept. Electrical Engineering
University of California, Santa Cruz
alyson@ucsc.edu

Sundeep Rangan
Dept. Electrical & Computer Engineering
New York University Polytechnic Institute
srangan@nyu.edu

Abstract

Fluorescent calcium imaging provides a potentially powerful tool for inferring connectivity in neural circuits with up to thousands of neurons. However, a key challenge in using calcium imaging for connectivity detection is that current systems often have a temporal response and frame rate that can be orders of magnitude slower than the underlying neural spiking process. Bayesian inference methods based on expectation-maximization (EM) have been proposed to overcome these limitations, but are often computationally demanding since the E-step in the EM procedure typically involves state estimation for a high-dimensional nonlinear dynamical system. In this work, we propose a computationally fast method for the state estimation based on a hybrid of loopy belief propagation and approximate message passing (AMP). The key insight is that a neural system as viewed through calcium imaging can be factorized into simple scalar dynamical systems for each neuron with linear interconnections between the neurons. Using the structure, the updates in the proposed hybrid AMP methodology can be computed by a set of one-dimensional state estimation procedures and linear transforms with the connectivity matrix. This yields a computationally scalable method for inferring connectivity of large neural circuits. Simulations of the method on realistic neural networks demonstrate good accuracy with computation times that are potentially significantly faster than current approaches based on Markov Chain Monte Carlo methods.

1 Introduction

Determining connectivity in populations of neurons is fundamental to understanding neural computation and function. In recent years, calcium imaging has emerged as a promising technique for measuring synaptic activity and mapping neural micro-circuits [1–5]. Fluorescent calcium-sensitive dyes and genetically-encoded calcium indicators can be loaded into neurons, which can then be imaged for spiking activity either *in vivo* or *in vitro*. Current methods enable imaging populations of hundreds to thousands of neurons with very high spatial resolution. Using two-photon microscopy, imaging can also be localized to specific depths and cortical layers [6]. Calcium imaging also has the potential to be combined with optogenetic stimulation techniques such as in [7].

However, inferring neural connectivity from calcium imaging remains a mathematically and computationally challenging problem. Unlike anatomical methods, calcium imaging does not directly measure connections. Instead, connections must be inferred indirectly from statistical relationships between spike activities of different neurons. In addition, the measurements of the spikes from calcium imaging are indirect and noisy. Most importantly, the imaging introduces significant temporal blurring of the spike times: the typical time constants for the decay of the fluorescent calcium concentration, $[Ca^{2+}]$, can be on the order of a second – orders of magnitude slower than the spike rates and inter-neuron dynamics. Moreover, the calcium imaging frame rate remains relatively slow –

often less than 100 Hz. Hence, determining connectivity typically requires super-resolution of spike times within the frame period.

To overcome these challenges, the recent work [8] proposed a Bayesian inference method to estimate functional connectivity from calcium imaging in a systematic manner. Unlike "model-free" approaches such as in [9], the method in [8] assumed a detailed functional model of the neural dynamics with unknown parameters including a connectivity weight matrix $\mathbf{W}$. The model parameters including the connectivity matrix can then be estimated via a standard EM procedure [10]. While the method is general, one of the challenges in implementing the algorithm is the computational complexity. As we discuss below, the E-step in the EM procedure essentially requires estimating the distributions of hidden states in a nonlinear dynamical system whose state dimension grows linearly with the number of neurons. Since exact computation of these densities grows exponentially in the state dimension, [8] uses an approximate method based on blockwise Gibbs sampling where each block of variables consists of the hidden states associated with one neuron. Since the variables within a block are described as a low-dimensional dynamical system, the updates of the densities for the Gibbs sampling can be computed efficiently via a standard particle filter [11, 12]. However, simulations of the method show that the mixing between blocks can still take considerable time to converge.

This paper presents two novel contributions that can potentially significantly improve the computation time of the EM estimation as well as the generality of the model.

The first contribution is to employ an approximate message passing (AMP) technique in the computationally difficult EM step. The key insight here is to recognize that a system with multiple neurons can be "factorized" into simple, scalar dynamical systems for each neuron with linear interactions between the neurons. As described below, we assume a standard leaky integrate-and-fire (LIF) model for each neuron [13] and a first-order AR process for the calcium imaging [14]. Under this model, the dynamics of N neurons can be described by $2N$ systems, each with a scalar (i.e. one-dimensional) state. The coupling between the systems will be linear as described by the connectivity matrix $\mathbf{W}$. Using this factorization, approximate state estimation can then be efficiently performed via approximations of loopy belief propagation (BP) [15]. Specifically, we show that the loopy BP updates at each of the factor nodes associated with the integrate-and-fire and calcium imaging can be performed via a scalar standard forward–backward filter. For the updates associated with the linear transform $\mathbf{W}$, we use recently-developed approximate message passing (AMP) methods.

AMP was originally proposed in [16] for problems in compressed sensing. Similar to expectation propagation [17], AMP methods use Gaussian and quadratic approximations of loopy BP but with further simplifications that leverage the linear interactions. AMP was used for neural mapping from multi-neuron excitation and neural receptive field estimation in [18, 19]. Here, we use a so-called hybrid AMP technique proposed in [20] that combines AMP updates across the linear coupling terms with standard loopy BP updates on the remainder of the system. When applied to the neural system, we show that the estimation updates become remarkably simple: For a system with N neurons, each iteration involves running $2N$ forward–backward scalar state estimation algorithms, along with multiplications by $\mathbf{W}$ and $\mathbf{W}^T$ at each time step. The practical complexity scales as $O(NT)$ where T is the number of time steps. We demonstrate that the method can be significantly faster than the blockwise Gibbs sampling proposed in [8], with similar accuracy.

In addition to the potential computational improvement, the AMP-based procedure is somewhat more general. For example, the approach in [8] assumes a generalized linear model (GLM) for the spike rate of each neuron. The approach in this work can be theoretically applied to arbitrary scalar dynamics that describe spiking. In particular, the approach can incorporate a physically more realistic LIF model.

The second contribution is a novel method for initial estimation of the connectivity matrix. Since we are applying the EM methodology to a fundamentally non-convex problem, the algorithm is sensitive to the initial condition. However, there are now several good approaches for initial estimation the spike times of each neuron from its calcium trace via sparse deconvolution [21–23]. We show that, under a leaky integrate and fire model, that if the true spike times were known exactly, then the maximum likelihood (ML) estimation of the connectivity matrix can be performed via sparse probit regression – a standard convex programming problem used in classification [24]. We propose to

obtain an initial estimate for the connectivity matrix $\mathbf{W}$ by applying the sparse probit regression to the initial estimate of the spike times.

2 System Model

We consider a recurrent network of N spontaneously firing neurons. All dynamics are approximated in discrete time with some time step Δ, with a typical value Δ = 1 ms. Importantly, this time step is typically smaller than the calcium imaging period, so the model captures the dynamics between observations. Time bins are indexed by $k = 0, \ldots, T-1$, where T is the number of time bins so that $T\Delta$ is the total observation time in seconds. Each neuron i generates a sequence of spikes (action potentials) indicated by random variables s_i^k taking values 0 or 1 to represent whether there was a spike in time bin k or not. It is assumed that the discretization step Δ is sufficiently small such that there is at most one action potential from a neuron in any one time bin. The spikes are generated via a standard leaky integrate-and-fire (LIF) model [13] where the (single compartment) membrane voltage v_i^k of each neuron i and its corresponding spike output sequence s_i^k evolve as

$$\tilde{v}_i^{k+1} = (1-\alpha_{IF})v_i^k + q_i^k + d_{v_i}^k, \quad q_i^k = \sum_{j=1}^{N} W_{ij} s_j^{k-\delta} + b_{IF,i}, \quad d_{v_i}^k \sim \mathcal{N}(0, \tau_{IF}), \tag{1}$$

and

$$(v_i^{k+1}, s_i^{k+1}) = \begin{cases} (\tilde{v}_i^k, 0) & \text{if } v_i^k < \mu, \\ (0,1) & \text{if } \tilde{v}_i^k \geq \mu, \end{cases} \tag{2}$$

where α_{IF} is a time constant for the integration leakage; μ is the threshold potential at which the neurons spikes; $b_{IF,i}$ is a constant bias term; q_i^k is the increase in the membrane potential from the pre-synaptic spikes from other neurons and $d_{v_i}^k$ is a noise term including both thermal noise and currents from other neurons that are outside the observation window. The voltage has been scaled so that the reset voltage is zero. The parameter δ is the integer delay (in units of the time step Δ) between the spike in one neuron and the increase in the membrane voltage in the post-synaptic neuron. An implicit assumption in this model is the post-synaptic current arrives in a single time bin with a fixed delay.

To determine functional connectivity, the key parameter to estimate will be the matrix $\mathbf{W}$ of the weighting terms W_{ij} in (1). Each parameter W_{ij} represents the increase in the membrane voltage in neuron i due to the current triggered from a spike in neuron j. The connectivity weight W_{ij} will be zero whenever neuron j has no connection to neuron i. Thus, determining $\mathbf{W}$ will determine which neurons are connected to one another and the strengths of those connections.

For the calcium imaging, we use a standard model [8], where the concentration of fluorescent Calcium has a fast initial rise upon an action potential followed by a slow exponential decay. Specifically, we let $z_i^k = [\text{Ca}^{2+}]_k$ be the concentration of fluorescent Calcium in neuron i in time bin k and assume it evolves as first-order auto-regressive $AR(1)$ model,

$$z_i^{k+1} = (1-\alpha_{CA,i})z_i^k + s_i^k, \tag{3}$$

where α_{CA} is the Calcium time constant. The observed net fluorescence level is then given by a noisy version of z_i^k,

$$y_i^k = a_{CA,i} z_i^k + b_{CA,i} + d_{y_i}^k, \quad d_{y_i}^k \sim \mathcal{N}(0, \tau_y), \tag{4}$$

where $a_{CA,i}$ and $b_{CA,i}$ are constants and d_{y_i} is white Gaussian noise with variance τ_y. Nonlinearities such as saturation described in [14] can also be modeled.

As mentioned in the Introduction, a key challenge in calcium imaging is the relatively slow frame rate which has the effect of subsampling of the fluorescence. To model the subsampling, we let I_F denote the set of time indices k on which we observe F_i^k. We will assume that fluorescence values are observed once every T_F time steps for some integer period T_F so that $I_F = \{0, T_F, 2T_F, \ldots, KT_F\}$ where K is the number of Calcium image frames.

3 Parameter Estimation via Message Passing

3.1 Problem Formulation

Let θ be set of all the unknown parameters,

$$\theta = \{\mathbf{W}, \tau_{IF}, \tau_{CA}, \alpha_{IF}, b_{IF,i}, \alpha_{CA}, a_{CA,i}, b_{CA,i}, i = 1, \ldots, N\}, \tag{5}$$

which includes the connectivity matrix, time constants and various variances and bias terms. Estimating the parameter set θ will provide an estimate of the connectivity matrix $\mathbf{W}$, which is our main goal.

To estimate θ, we consider a regularized maximum likelihood (ML) estimate

$$\widehat{\theta} = \arg\max_{\theta} L(\mathbf{y}|\theta) + \phi(\theta), \quad L(\mathbf{y}|\theta) = -\log p(\mathbf{y}|\theta), \tag{6}$$

where $\mathbf{y}$ is the set of observed values; $L(\mathbf{y}|\theta)$ is the negative log likelihood of $\mathbf{y}$ given the parameters θ and $\phi(\theta)$ is some regularization function. For the calcium imaging problem, the observations $\mathbf{y}$ are the observed fluorescence values across all the neurons,

$$\mathbf{y} = \{\mathbf{y}_1, \ldots, \mathbf{y}_N\}, \quad \mathbf{y}_i = \left\{y_i^k, \quad k \in I_F\right\}, \tag{7}$$

where $\mathbf{y}_i$ is the set of fluorescence values from neuron i, and, as mentioned above, I_F is the set of time indices k on which the fluorescence is sampled.

The regularization function $\phi(\theta)$ can be used to impose constraints or priors on the parameters. In this work, we will assume a simple regularizer that only constrains the connectivity matrix $\mathbf{W}$,

$$\phi(\theta) = \lambda\|\mathbf{W}\|_1, \quad \|\mathbf{W}\|_1 := \sum_{ij} |W_{ij}|, \tag{8}$$

where λ is a positive constant. The ℓ_1 regularizer is a standard convex function used to encourage sparsity [25], which we know in this case must be valid since most neurons are not connected to one another.

3.2 EM Estimation

Exact computation of $\widehat{\theta}$ in (6) is generally intractable, since the observed fluorescence values $\mathbf{y}$ depend on the unknown parameters θ through a large set of hidden variables. Similar to [8], we thus use a standard EM procedure [10]. To apply the EM procedure to the calcium imaging problem, let $\mathbf{x}$ be the set of hidden variables,

$$\mathbf{x} = \{\mathbf{v}, \mathbf{z}, \mathbf{q}, \mathbf{s}\}, \tag{9}$$

where $\mathbf{v}$ are the membrane voltages of the neurons, $\mathbf{z}$ the calcium concentrations, $\mathbf{s}$ the spike outputs and $\mathbf{q}$ the linearly combined spike inputs. For any of these variables, we will use the subscript i (e.g. $\mathbf{v}_i$) to denote the values of the variables of a particular neuron i across all time steps and superscript k (e.g. $\mathbf{v}^k$) to denote the values across all neurons at a particular time step k. Thus, for the membrane voltage

$$\mathbf{v} = \left\{v_i^k\right\}, \quad \mathbf{v}^k = \left(v_1^k, \ldots, v_N^k\right), \quad \mathbf{v}_i = \left(v_i^0, \ldots, v_i^{T-1}\right).$$

The EM procedure alternately estimates distributions on the hidden variables $\mathbf{x}$ given the current parameter estimate for θ (the E-step); and then updates the estimates for parameter vector θ given the current distribution on the hidden variables $\mathbf{x}$ (the M-step).

- *E-Step:* Given parameter estimates $\widehat{\theta}^\ell$, estimate

  $$P(\mathbf{x}|\mathbf{y}, \widehat{\theta}^\ell), \tag{10}$$

  which is the posterior distribution of the hidden variables $\mathbf{x}$ given the observations $\mathbf{y}$ and current parameter estimate $\widehat{\theta}^\ell$.

- *M-step* Update the parameter estimate via the minimization,

$$\widehat{\theta}^{\ell+1} = \arg\min_{\theta} \mathbb{E}\left[L(\mathbf{x}, \mathbf{y}|\theta)|\widehat{\theta}^{\ell}\right] + \phi(\theta), \tag{11}$$

where $L(\mathbf{x}, \mathbf{y}|\theta)$ is the joint negative log likelihood,

$$L(\mathbf{x}, \mathbf{y}|\theta) = -\log p(\mathbf{x}, \mathbf{y}|\theta). \tag{12}$$

In (11) the expectation is with respect to the distribution found in (10) and $\phi(\theta)$ is the parameter regularization function.

The next two sections will describe how we approximately perform each of these steps.

3.3 E-Step estimation via Approximate Message Passing

For the calcium imaging problem, the challenging step of the EM procedure is the E-step, since the hidden variables $\mathbf{x}$ to be estimated are the states and outputs of a high-dimensional nonlinear dynamical system. Under the model in Section 2, a system with N neurons will require N states for the membrane voltages v_i^k and N states for the bound Ca concentration levels z_i^k, resulting in a total state dimension of $2N$. The E-step for this system is essentially a state estimation problem, and exact inference of the states of a general nonlinear dynamical system grows exponentially in the state dimension. Hence, exact computation of the posterior distribution (10) for the system will be intractable even for a moderately sized network.

As described in the Introduction, we thus use an approximate messaging passing method that exploits the separable structure of the system. For the remainder of this section, we will assume the parameters θ in (5) are fixed to the current parameter estimate $\widehat{\theta}^{\ell}$. Then, under the assumptions of Section 2, the joint probability distribution function of the variables can be written in a factorized form,

$$P(\mathbf{x}, \mathbf{y}) = P(\mathbf{q}, \mathbf{v}, \mathbf{s}, \mathbf{z}, \mathbf{y}) = \frac{1}{Z} \prod_{k=0}^{T-1} \mathbb{1}_{\{\mathbf{q}^k = \mathbf{W}\mathbf{s}^k\}} \prod_{i=1}^{N} \psi_i^{IF}(\mathbf{q}_i, \mathbf{v}_i, \mathbf{s}_i) \psi_i^{CA}(\mathbf{s}_i, \mathbf{z}_i, \mathbf{y}_i), \tag{13}$$

where Z is a normalization constant; $\psi_i^{IF}(\mathbf{q}_i, \mathbf{v}_i, \mathbf{s}_i)$ is the potential function relating the summed spike inputs $\mathbf{q}_i$ to the membrane voltages $\mathbf{v}_i$ and spike outputs $\mathbf{s}_i$; $\psi_i^{CA}(\mathbf{s}_i, \mathbf{z}_i, \mathbf{y}_i)$ relates the spike outputs $\mathbf{s}_i$ to the bound calcium concentrations $\mathbf{z}_i$ and observed fluorescence values $\mathbf{y}_i$; and the term $\mathbb{1}_{\{\mathbf{q}^k = \mathbf{W}\mathbf{s}^k\}}$ indicates that the distribution is to be restricted to the set satisfying the linear constraints $\mathbf{q}^k = \mathbf{W}\mathbf{s}^k$ across all time steps k.

As in standard loopy BP [15], we represent the distribution (13) in a *factor graph* as shown in Fig. 1. Now, for the E-step, we need to compute the marginals of the posterior distribution $p(\mathbf{x}|\mathbf{y})$ from the joint distribution (13). Using the factor graph representation, loopy BP iteratively updates estimates of these marginal posterior distributions using a message passing procedure, where the estimates of the distributions (called beliefs) are passed between the variable and factor nodes in the graph.

To reduce the computations in loopy BP further, we employ an approximate message passing (AMP) method for the updates in the factor node corresponding to the linear constraints $\mathbf{q}^k = \mathbf{W}\mathbf{s}^k$. AMP was originally developed in [16] for problems in compressed sensing, and can be derived as Gaussian approximations of loopy BP [26, 27] similar to expectation propagation [28]. In this work, we employ a hybrid form of AMP [20] that combines AMP with standard message passing. The AMP methods have the benefit of being computationally very fast and, for problems with certain large random transforms, the methods can yield provably Bayes-optimal estimates of the posteriors, even in certain non-convex problem instances. However, similar to standard loopy BP, the AMP and its variants may diverge for general transforms (see [29–31] for some discussion of the convergence). For our problem, we will see in simulations that we obtain fast convergence in a relatively small number of iterations.

We provide some details of the hybrid AMP method in Appendix A, but the basic procedure for the factor node updates and the reasons why these computations are simple can be summarized as follows. At a high level, the factor graph structure in Fig. 1 partitions the $2N$-dimensional nonlinear dynamical system into N scalar systems associated with each membrane voltage v_i^k and an

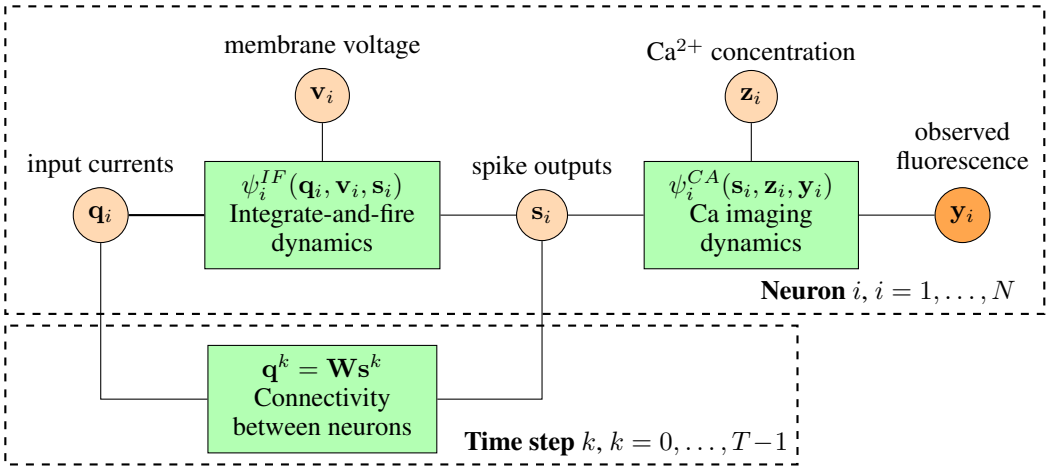

Figure 1: Factor graph plate representation of the system where the spike dynamics are described by the factor node $\psi_i^{IF}(\mathbf{q}_i, \mathbf{v}_i, \mathbf{s}_i)$ and the calcium image dynamics are represented via the factor node $\psi_i^{CA}(\mathbf{s}_i, \mathbf{z}_i, \mathbf{y}_i)$. The high-dimensional dynamical system is described as $2N$ scalar dynamical systems (2 for each neuron) with linear interconnections, $\mathbf{q}^k = \mathbf{W}\mathbf{s}^k$ between the neurons. A computational efficient approximation of loopy BP [20] is applied to this graph for approximate Bayesian inference required in the E-step of the EM algorithm.

additional N scalar systems associated with each calcium concentration level z_i^k. The only coupling between these systems is through the linear relationships $\mathbf{q}^k = \mathbf{W}\mathbf{s}^k$. As shown in Appendix A, on each of the scalar systems, the factor node updates required by loopy BP essentially reduces to a state estimation problem for this system. Since the state space of this system is scalar (i.e. one-dimensional), we can discretize the state space well with a small number of points – in the experiments below we use $L = 20$ points per dimension. Once discretized, the state estimation can be performed via a standard forward–backward algorithm. If there are T time steps, the algorithm will have a computational cost of $O(TL^2)$ per scalar system. Hence, all the factor node updates across all the $2N$ scalar systems has total complexity $O(NTL^2)$.

For the factor nodes associated with the linear constraints $\mathbf{q}^k = \mathbf{W}\mathbf{s}^k$, we use the AMP approximations [20]. In this approximation, the messages for the transform outputs q_i^k are approximated as Gaussians which is, at least heuristically, justified since the they are outputs of a linear transform of a large number of variables, s_i^k. In the AMP algorithm, the belief updates for the variables $\mathbf{q}^k$ and $\mathbf{s}^k$ can then be computed simply by linear transformations of $\mathbf{W}$ and $\mathbf{W}^T$. Since $\mathbf{W}$ represents a connectivity matrix, it is generally sparse. If each row of $\mathbf{W}$ has d non-zero values, multiplication by $\mathbf{W}$ and $\mathbf{W}^T$ will be $O(Nd)$. Performing the multiplications across all time steps results in a total complexity of $O(NTd)$.

Thus, the total complexity of the proposed E-step estimation method is $O(NTL^2 + NTd)$ per loopy BP iteration. We typically use a small number of loopy BP iterations per EM update (in fact, in the experiments below, we found reasonable performance with one loopy BP update per EM update). In summary, we see that while the overall neural system is high-dimensional, it has a linear + scalar structure. Under the assumption of the bounded connectivity d, this structure enables an approximate inference strategy that scales linearly with the number of neurons N and time steps T. Moreover, the updates in different scalar systems can be computed separately allowing a readily parallelizable implementation.

3.4 Approximate M-step Optimization

The M-step (11) is computationally relatively simple. All the parameters in θ in (5) have a linear relationship between the components of the variables in the vector $\mathbf{x}$ in (9). For example, the parameters $a_{CA,i}$ and $b_{CA,i}$ appear in the fluorescence output equation (4). Since the noise $d_{y_i}^k$ in this

equation is Gaussian, the negative log likelihood (12) is given by

$$L(\mathbf{x}, \mathbf{y}|\theta) = \frac{1}{2\tau_{y_i}} \sum_{k \in I_F} (y_i^k - a_{CA,i} z_i^k - b_{CA,i})^2 + \frac{T}{2} \log(\tau_{y_i}) + \text{other terms},$$

where "other terms" depend on parameters other than $a_{CA,i}$ and $b_{CA,i}$. The expectation $\mathbb{E}(L(\mathbf{x}, \mathbf{y}|\theta)|\widehat{\theta}^\ell)$ will then depend only on the mean and variance of the variables y_i^k and z_i^k, which are provided by the E-step estimation. Thus, the M-step optimization in (11) can be computed via a simple least-squares problem. Using the linear relation (1), a similar method can be used for $\alpha_{IF,i}$ and $b_{IF,i}$, and the linear relation (3) can be used to estimate the calcium time constant α_{CA}.

To estimate the connectivity matrix $\mathbf{W}$, let $\mathbf{r}^k = \mathbf{q}^k - \mathbf{W}\mathbf{s}^k$ so that the constraints in (13) is equivalent to the condition that $\mathbf{r}^k = 0$. Thus, the term containing $\mathbf{W}$ in the expectation of the negative log likelihood $\mathbb{E}(L(\mathbf{x}, \mathbf{y}|\theta)|\widehat{\theta}^\ell)$ is given by the negative log probability density of $\mathbf{r}^k$ evaluated at zero. In general, this density will be a complex function of $\mathbf{W}$ and difficult to minimize. So, we approximate the density as follows: Let $\widehat{\mathbf{q}}$ and $\widehat{\mathbf{s}}$ be the expectation of the variables $\mathbf{q}$ and $\mathbf{s}$ given by the E-step. Hence, the expectation of $\mathbf{r}^k$ is $\widehat{\mathbf{q}}^k - \mathbf{W}\widehat{\mathbf{s}}^k$. As a simple approximation, we will then assume that the variables r_i^k are Gaussian, independent and having some constant variance σ^2. Under this simplifying assumption, the M-step optimization of $\mathbf{W}$ with the ℓ_1 regularizer (8) reduces to

$$\widehat{\mathbf{W}} = \arg\min_{\mathbf{W}} \frac{1}{2} \sum_{k=0}^{T-1} \|\widehat{\mathbf{q}}^k - \mathbf{W}\widehat{\mathbf{s}}^k\|^2 + \sigma^2 \lambda \|\mathbf{W}\|_1, \tag{14}$$

For a given value of $\sigma^2\lambda$, the optimization (14) is a standard LASSO optimization [32] which can be evaluated efficiently via a number of convex programming methods. In this work, in each M-step, we adjust the regularization parameter $\sigma^2\lambda$ to obtain a desired fixed sparsity level in the solution $\mathbf{W}$.

3.5 Initial Estimation via Sparse Regression

Since the EM algorithm cannot be guaranteed to converge a global maxima, it is important to pick the initial parameter estimates carefully. The time constants and noise levels for the calcium image can be extracted from the second-order statistics of fluorescence values and simple thresholding can provide a coarse estimate of the spike rate.

The key challenge is to obtain a good estimate for the connectivity matrix $\mathbf{W}$. For each neuron i, we first make an initial estimate of the spike probabilities $P(s_i^k = 1|\mathbf{y}_i)$ from the observed fluorescence values $\mathbf{y}_i$, assuming some i.i.d. prior of the form $P(s_i^t) = \lambda\Delta$, where λ is the estimated average spike rate per second. This estimation can be solved with the filtering method in [14] and is also equivalent to the method we use for the factor node updates. We can then threshold these probabilities to make a hard initial decision on each spike: $s_i^k = 0$ or 1.

We then propose to estimate $\mathbf{W}$ from the spikes as follows. Fix a neuron i and let $\mathbf{w}_i$ be the vector of weights W_{ij}, $j = 1, \ldots, N$. Under the assumption that the initial spike sequence s_i^k is exactly correct, it is shown in Appendix B that a regularized maximum likelihood estimate of $\mathbf{w}_i$ and bias term $b_{IF,i}$ is given by

$$(\widehat{\mathbf{w}}_i, \widehat{b}_{IF,i}) = \arg\min_{\mathbf{w}_i, b_{IF,i}} \sum_{k=0}^{T-1} L_{ik}(\mathbf{u}_k^T \mathbf{w}_i + c_{ik} b_{IF,i} - \mu, s_i^k) + \lambda \sum_{j=1}^{N} |W_{ij}|, \tag{15}$$

where L_{ik} is a probit loss function and the vector $\mathbf{u}_k$ and scalar c_{ik} can be determined from the spike estimates. The optimization (15) is precisely a standard probit regression used in sparse linear classification [24]. This form arises due to the nature of the leaky integrate-and-fire model (1) and (2). Thus, assuming the initial spike sequences are estimated reasonably accurately, one can obtain good initial estimates for the weights W_{ij} and bias terms $b_{IF,i}$ by solving a standard classification problem.

We point out that [33] has recently provided an alternative method for recovery of connectivity matrix from the spikes assuming a LIF model based on maximizing information flow.

Parameter	**Value**
Number of neurons, N	100
Connection sparsity	10% with random connections. All connections are excitatory with the non-zero weights W_{ij} being exponentially distributed.
Mean firing rate per neuron	10 Hz
Simulation time step, Δ	1 ms
Total simulation time, $T\Delta$	10 sec (10,000 time steps)
Integration time constant, α_{IF}	20 ms
Conduction delay, δ	2 time steps = 2 ms
Integration noise, $d_{v_i}^k$	Produced from two unobserved neurons.
Ca time constant, α_{CA}	500 ms
Fluorescence noise, τ_{CA}	Set to 20 dB SNR
Ca frame rate , $1/T_F$	100 Hz

Table 1: Parameters for the Ca image simulation.

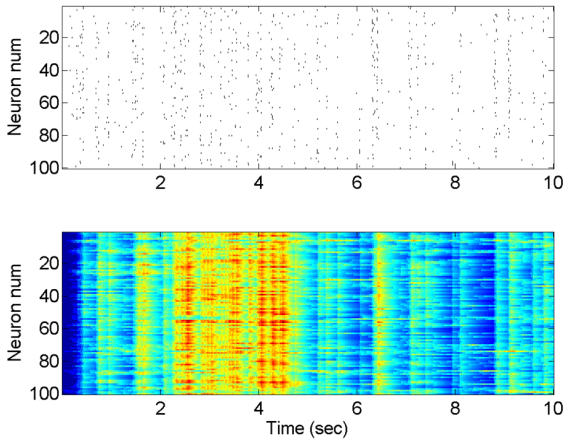

Figure 2: Typical network simulation trace. Top panel: Spike traces for the 100 neuron simulated network. Bottom panel: Calcium image fluorescence levels. Due to the random network topology, neurons often fire together, significantly complicating connectivity detection. Also, as seen in the lower panel, the slow decay of the fluorescent calcium blurs the spikes in the calcium image.

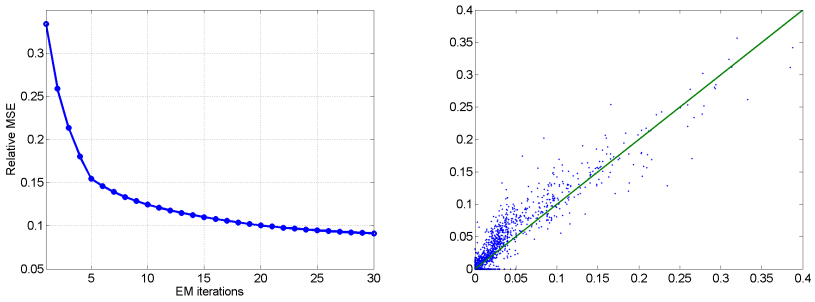

Figure 3: Weight estimation accuracy. Left: Normalized mean-squared error as a function of the iteration number. Right: Scatter plot of the true and estimated weights.

4 Numerical Example

The method was tested using realistic network parameters, as shown in Table 1, similar to those found in neurons networks within a cortical column [34]. Similar parameters are used in [8]. The network consisted of 100 neurons with each neuron randomly connected to 10% of the other neurons. The non-zero weights W_{ij} were drawn from an exponential distribution. All weights were positive (i.e. the neurons were excitatory – there were no inhibitory neurons in the simulation). However, inhibitory neurons can also be added. A typical random matrix $\mathbf{W}$ generated in this manner would not in general result in a stable system. To stabilize the system, we followed the procedure in [9] where the system is simulated multiple times. After each simulation, the rows of the matrix $\mathbf{W}$ were adjusted up or down to increase or decrease the spike rate until all neurons spiked at a desired target rate. In this case, we assumed a desired average spike rate of 10 Hz.

From the parameters in Table 1, we can immediately see the challenges in the estimation. Most importantly, the calcium imaging time constant α_{CA} is set for 500 ms. Since the average neurons spike rate is assumed to be 10 Hz, several spikes will typically appear within a single time constant. Moreover, both the integration time constant and inter-neuron conduction time are much smaller than both the image frame rate and Calcium time constants.

A typical simulation of the network after the stabilization is shown in Fig. 2. Observe that due to the random connectivity, spiking in one neuron can rapidly cause the entire network to fire. This appears as the vertical bright stripes in the lower panel of Fig. 2. This synchronization makes the connectivity detection difficult to detect under temporal blurring of Ca imaging since it is hard to determine which neuron is causing which neuron to fire. Thus, the random matrix is a particularly challenging test case.

The results of the estimation are shown in Fig. 3. The left panel shows the relative mean squared error defined as

$$\text{relative MSE} = \frac{\min_\alpha \sum_{ij} |W_{ij} - \alpha \widehat{W}_{ij}|^2}{\sum_{ij} |W_{ij}|^2}, \tag{16}$$

where $\widehat{W}_{ij}$ is the estimate for the weight W_{ij}. The minimization over all α is performed since the method can only estimate the weights up to a constant scaling. The relative MSE is plotted as a function of the EM iteration, where we have performed only a single loopy BP iteration for each EM iteration. We see that after only 30 iterations we obtain a relative MSE of 7% – a number at least comparable to earlier results in [8], but with significantly less computation. The right panel shows a scatter plot of the estimated weights $\widehat{W}_{ij}$ against the true weights W_{ij}.

5 Conclusions

We have presented a scalable method for inferring connectivity in neural systems from calcium imaging. The method is based on factorizing the systems into scalar dynamical systems with linear connections. Once in this form, state estimation – the key computationally challenging component of the EM estimation – is tractable via approximating message passing methods. The key next step

in the work is to test the methods on real data and also provide more comprehensive computational comparisons against current techniques such as [8].

A E-Step Message Passing Implementation Details

As described in Section 3.3, the E-step inference is performed via an approximate message passing technique [20]. As in standard sum-product loopy BP [15], the algorithm is based on passing "belief messages" between the variable and factor nodes representing estimates of the posterior marginals of the variables. Referring to the factor graph in Fig. 1, we will use the subscripts IF, CA and W to refer respectively to the factor nodes for integrate and fire potential functions ψ_i^{IF}, the calcium imaging potential functions ψ_i^{CA} and the linear constraints $\mathbf{q}^k = \mathbf{W}\mathbf{s}^k$. We use the subscripts Q and S to refer to the variable nodes for $\mathbf{q}$ and $\mathbf{s}$. We use the notation such as $P_{IF\to Q}(q_i^k)$ to denote the belief message to the variable node q_i^k from the integrate and factor node ψ_i^{IF}. Similarly, $P_{IF\leftarrow Q}(q_i^k)$ will denote the reverse message from the variable node to the factor node.

The messages to and from the variable nodes s_i^k are binary: $s_i^k = 0$ or 1. Hence, they can be parameterized by a single scalar. Similar to expectation propagation [17], the messages to and from the variable nodes q_i^k are approximated as Gaussians, so that we only need to maintain the first and second moments. Gaussian approximations are used in the variational Bayes method for calcium imaging inference in [35].

To apply the hybrid AMP algorithm of [20] to the factor graph in Fig. 1, we use standard loopy BP message updates on the IF and CA factor nodes, and AMP updates on the linear constraints $\mathbf{q}^k = \mathbf{W}\mathbf{s}^k$. The AMP updates are based on linear-Gaussian approximations. The details of the messages updates are as follows.

Messages from ψ_i^{IF}: This factor node represents the integrate and fire system for the voltages v_i^k and is given by

$$\psi_i^{IF}(\mathbf{q}_i, \mathbf{v}_i, \mathbf{s}_i) = \prod_{k=0}^{T-1} P(v_i^{k+1}, s_i^{k+1} | v_i^k, q_i^k), \tag{17}$$

where the conditional density $P(v_i^{k+1}, s_i^{k+1}|v_i^k, q_i^k)$ is given by integrate and fire system (1) and (2). To describe the output belief propagation messages for this factor node, define the joint distribution,

$$\begin{aligned} P(\mathbf{q}_i, \mathbf{v}_i, \mathbf{s}_i) &\propto \psi_i^{IF}(\mathbf{q}_i, \mathbf{v}_i, \mathbf{s}_i) P_{IF\leftarrow Q}(q_i^k) P_{IF\leftarrow S}(s_i^k) \\ &= \prod_{k=0}^{T-1} P(v_i^{k+1}, s_i^{k+1}|v_i^k, q_i^k) P_{IF\leftarrow Q}(q_i^k) P_{IF\leftarrow S}(s_i^k), \end{aligned} \tag{18}$$

where $P_{IF\leftarrow Q}(q_i^k)$ and $P_{IF\leftarrow S}(s_i^k)$ are the incoming messages from the variable nodes. To compute the output messages, we must first compute the marginal densities $P(q_i^k)$ and $P(s_i^k)$ of this joint distribution (18).

To compute these marginal densities, define $\xi_i^k = q_i^k + d_{v_i}^k + b_i$. Now recall that the AMP assumption is that each incoming distribution $P_{IF\leftarrow Q}(q_i^k)$ is Gaussian. Let $\widehat{q}_i^k$ and $\tau_{q_i}^k$ be the mean and variance of this distribution. Thus, the joint distribution (18) is identical to the posterior distribution of a linear system with a Gaussian input

$$\tilde{v}_i^k = (1-\alpha_{IF})\tilde{v}_i^k + \xi_i^k, \quad \xi_i^k \sim \mathcal{N}(\widehat{q}_i^k + b_i, \tau_{q_i}^k + \tau_{IF}), \tag{19}$$

with the reset and spike output in (2) and output observations $P(s_i^k|\phi_i^k)$. This is a nonlinear system with a one-dimensional state v_i^k. Hence, one can, in principle, approximately compute the marginal densities $P(q_i^k)$ and $P(s_i^k)$ of (18) with a one-dimensional particle filter [12]. However, we found it computationally faster to simply use a fixed discretization of the set of values v_i^k. In the experiments below we used $L = 20$ values linearly spaced from 0 to the threshold level μ. Using the fixed discretization enables a number of the computations to be computed once for all time steps, and also removes the computations and logic for pruning necessary in particle filtering. After computing the marginals $P(q_i^k)$ and $P(s_i^k)$, we set the output messages as

$$P_{IF\to Q}(q_i^k) \propto P(q_i^k)/P_{IF\leftarrow Q}(q_i^k), \quad P_{IF\to S}(s_i^k) \propto P(s_i^k)/P_{IF\leftarrow S}(s_i^k).$$

Messages from ψ_i^{CA}: In this case, the factor node represents the Ca imaging dynamics and is given by,

$$\psi_i^{CA}(\mathbf{s}_i, \mathbf{z}_i, \mathbf{y}_i) = \prod_{k=0}^{T-1} P(z_i^{k+1}|z_i^k, s_i^k) \prod_{k\in I_F} P(y_i^k|z_i^k), \tag{20}$$

where $P(z_i^{k+1}|z_i^k, s_i^k)$ and $P(y_i^k|z_i^k)$ are given by the relations (3) and (4) describing the fluorescent Ca^{2+} concentration evolution and observed fluorescence. Recall that I_F in (20) is the set of time samples on which the output y_i^k is observed. To compute the output beliefs for the factor node, as before, we define the joint distribution,

$$\begin{aligned} P(\mathbf{s}_i, \mathbf{z}_i, \mathbf{y}_i) &\propto \psi_i^{CA}(\mathbf{s}_i, \mathbf{z}_i, \mathbf{y}_i) \prod_{k=0}^{T-1} P_{CA\leftarrow S}(s_i^k) \\ &= \prod_{k=0}^{T-1} P(z_i^{k+1}|z_i^k, s_i^k) P_{CA\leftarrow S}(s_i^k) \prod_{k\in I_F} P(y_i^k|z_i^k), \end{aligned} \tag{21}$$

where $P_{CA\leftarrow S}(s_i^k)$ are the input messages from the variable nodes s_i^k. This distribution $P(\mathbf{s}_i, \mathbf{z}_i, \mathbf{y}_i)$ is identical to a the distribution for a linear system with a scalar state z_i^k, Gaussian observations y_i^k and a discrete zero-one input s_i^k with prior $P_{CA\leftarrow S}(s_i^k)$. Similar to the integrate-and-fire case, we can approximately compute the posterior marginals $P(s_i^k|\mathbf{y}_i)$ by discretizing the states z_i^k and using a standard forward–backward estimator. From the posterior marginals $P(s_i^k|\mathbf{y}_i)$, we can then compute the belief messages for the factor node back to the variable nodes s_i^k: $P_{CA\to S}(s_i^k) \propto P(s_i^k|\mathbf{y}_i)/P_{CA\leftarrow S}(s_i^k)$.

AMP messages from the linear constraints $\mathbf{q}^k = \mathbf{W}\mathbf{s}^k$: Standard loopy BP updates for this factor node would be intractable for typical connectivity matrices $\mathbf{W}$. To see this, suppose that in the current estimate for the connection matrix $\mathbf{W}$, each neuron is connected to d other neurons. Hence the rows of $\mathbf{W}$ will have d non-zero entries. Each constraints $q_i^k = (\mathbf{W}\mathbf{s}^k)_i$ will thus involve d binary variables, and the complexity of the loopy BP update will then require $O(2^d)$ operations. This computation will be difficult for large d.

The hybrid AMP algorithm of [20] uses Gaussian approximations on the messages to reduce the computations to simple linear transforms. First consider the output messages $P_{W\to Q}(q_i^k)$ to the variable nodes q_i^k. These messages are Gaussians. Let $\widehat{q}_i^k$ and $\tau_{q_i^k}$ be their mean and variance and let $\widehat{\mathbf{q}}^k$ and τ_q^k be the vector of these quantities. In the hybrid AMP algorithm, these means and variances are given by

$$\widehat{\mathbf{q}}^k = \mathbf{W}\widehat{\mathbf{s}}^k - \boldsymbol{\tau}_q^k \mathbf{p}^k, \quad \boldsymbol{\tau}_q^k = |\mathbf{W}|^2 \boldsymbol{\tau}_s^k, \tag{22}$$

where $\widehat{\mathbf{s}}^k$ and $\boldsymbol{\tau}_s^k$ are the vectors of means and variances from the incoming messages $P_{W\leftarrow S}(s_i^k)$, and $|\mathbf{W}|^2$ is the matrix with components $|W_{ij}|^2$. The variables $\mathbf{p}^k$ is a real-valued state vector, which is initialized to zero. In (22), the multiplication $\boldsymbol{\tau}_q^k \mathbf{p}^k$ is to be performed componentwise: $\boldsymbol{\tau}_q^k \mathbf{p}^k)_i = \tau_{q_i^k} p_i^k$.

To process the incoming belief messages from the variable nodes $\mathbf{q}^k$, let $\overline{\mathbf{q}}^k$ and $\overline{\boldsymbol{\tau}}_q^k$ be the vector of mean and variances of the incoming beliefs $P_{W\leftarrow Q}(q_i^k)$. These quantities are to be distinguished from $\widehat{\mathbf{q}}^k$ and τ_q^k, the mean and variance vectors of the outgoing messages $P_{W\to Q}(q_i^k)$. We then first compute,

$$\mathbf{p}^k = (\overline{\mathbf{q}}^k - \widehat{\mathbf{q}}^k)/\boldsymbol{\tau}_q^k, \quad \boldsymbol{\tau}_p^k = \frac{1}{\boldsymbol{\tau}_q^k}\left[1 - \frac{\overline{\boldsymbol{\tau}}_q^k}{\boldsymbol{\tau}_q^k}\right], \tag{23}$$

where the divisions are componentwise. Next, we compute the quantities

$$\overline{\mathbf{s}}^k = \mathbf{s}^k + \boldsymbol{\tau}_s^k \mathbf{W}^T \mathbf{p}^k, \quad \overline{\boldsymbol{\tau}}_s^k = 1/(|\mathbf{W}|^2 \boldsymbol{\tau}_p^k), \tag{24}$$

where, again, the divisions are componentwise and the multiplication between $\boldsymbol{\tau}_s^k$ and $\mathbf{W}^T\mathbf{p}^k$ is componentwise. The output message to the variable nodes s_i^k is then given by

$$P_{W\to S}(s_i^k) \propto \exp\left(-\frac{1}{2\overline{\tau}_{s_i^k}}(s_i^k - \overline{s}_i^k)^2\right),$$

with possible values $s_i^k = 0$ or 1.

Variable node updates: The variable node updates are based on the standard sum-product rule [15]. In the factor graph in Fig. 1, each variable nodes q_i^k is only connected to two factor nodes: the factor node for the potential function ψ_i^{IF} and the factor node for the linear constraint $\mathbf{q}^k = \mathbf{W}\mathbf{s}^k$. Hence, the variable node will simply relay the messages between the nodes:

$$P_{IF\leftarrow Q}(q_i^k) = P_{W\rightarrow Q}(q_i^k), \quad P_{IF\leftarrow W}(q_i^k) = P_{W\rightarrow IF}(q_i^k),$$

Recall that these messages are approximated as Gaussians, so the messages can be represented by mean and variances.

Each binary spike variable nodes s_i^k is connected to three factor nodes: the integrate and fire potential function ψ_i^{IF}, the calcium imaging potential function ψ_i^{CA} and the linear constraint $\mathbf{q}^k = \mathbf{W}\mathbf{s}^k$. In the sum-product rule, the output message to any one of these nodes is the product of the incoming messages from the other two. Hence,

$$P_{IF\leftarrow S}(s_i^k) \propto P_{W\rightarrow S}(s_i^k)P_{Q\rightarrow S}(s_i^k), \quad P_{CA\leftarrow S}(s_i^k) \propto P_{W\rightarrow S}(s_i^k)P_{IF\rightarrow S}(s_i^k),$$
$$P_{W\leftarrow S}(s_i^k) \propto P_{CA\rightarrow S}(s_i^k)P_{IF\rightarrow S}(s_i^k).$$

The proportionality constant is simple to compute since the variables are binary so that $s_i^k = 0$ or 1.

B Initial Estimation of W via Sparse Probit Regression

We show that given the spike sequence s_i^k, the maximum likelihood estimate of the connectivity weights $\mathbf{W}$ and bias terms $b_{IF,i}$ can be computed approximately via a sparse probit regression of the form (15). To this end, suppose that we know the true spike sequence s_i^k for all neurons i and times k. Let $\{t_i^\ell, \ell = 1, \ldots, L_i\}$, be the index of time bins k where there is a spike (i.e. $s_i^k = 1$ when $k = t_i^\ell$ for some ℓ). Now, consider any time k between two spikes $k \in [t_i^\ell, t_i^{\ell+1})$. Since $s_i^k = 1$ at the initial time $k = t_i^\ell$, (2) shows that the voltage must starts at zero: $v_i^k = 0$. Integrating (1) from this initial condition, we have that for any $k \in (t_i^\ell, t_i^{\ell+1})$,

$$\tilde{v}_i^k = \sum_{j=1}^N W_{ij}u_j^k + (k - t_i^\ell)b_{IF,i} + \xi_i^k, \quad u_j^k = \sum_{m=0}^{k-t_i^\ell-1} (1-\alpha_{IF})^m s_i^{k-m-\delta}, \tag{25}$$

where ξ_i^k is the integration of the Gaussian noise $d_{v_i}^k$ up to time k. We can rewrite (25) in vector form

$$\tilde{v}_i^k = \mathbf{u}_k^T\mathbf{w}_i + c_{ik}b_{IF,i} + \xi_i^k, \tag{26}$$

where $\mathbf{u}_k$ and $\mathbf{w}_i$ are the vectors with the components W_{ij} and u_j^k and $c_{ik} = k - t_i^\ell$.

Now, let $\mathcal{A}^k$ be the set of spikes s_j^m for all j and all time bins $m \le k$, so that $\mathcal{A}_k$ represents the past spike events. Observe that in the model (26), the vector $\mathbf{u}_k$ can be computed from $\mathcal{A}_k$ and the noise ξ_i^k is independent of $\mathcal{A}^k$. Also, from (2), $s_i^{k+1} = 1$ if and only if $\tilde{v}_i^k \ge \mu$. Hence, we have that the conditional probability of the spike event at some time $k+1$, given the past spikes is

$$P(s_i^{k+1} = 1|\mathcal{A}_k) = \Phi\left(\frac{\mathbf{u}_k^T\mathbf{w}_i + c_{ik}b_{IF,i} - \mu}{\sigma_{ik}}\right), \tag{27}$$

where σ_{ik}^2 is the variance of ξ_i^k in (26), and $\Phi(z)$ is the cumulative distribution function of a unit Gaussian. Given the conditional probability (27), we can then estimate the parameters $\boldsymbol{\beta}$, through the maximization

$$(\widehat{\mathbf{w}}_i, \widehat{b}_{IF,i}) = \underset{\mathbf{w}_i, b_{IF,i}}{\arg\min} \sum_{k=0}^{T-1} L_{ik}(\mathbf{u}_k^T\mathbf{w}_i + c_{ik}b_{IF,i} - \mu, s_i^k) + \lambda\sum_{j=1}^N |W_{ij}|, \tag{28}$$

where $L_{ij}(z,s)$ is the probit loss function

$$L_{ik}(z,s) = \begin{cases} -\log(\Phi(z/\sigma_{ik})) & s_i^k = 1 \\ -\log(1-\Phi(z/\sigma_{ik})) & s_i^k = 0 \end{cases} \tag{29}$$

Given the conditional probabilities (27), the minimization (28) is precisely the maximum likelihood estimate of the parameters with an additional ℓ_1 regularization term to encourage sparsity in the weights $\mathbf{w}_i$. But this minimization is exactly a sparse probit regression that is standard in linear classification [24].

The only issue is that the optimization function (28) with the probit loss (29) requires knowledge of the threshold μ and variances σ_{ik}^2. Since we are only interested in the connectivity weights up to a constant factor, we can arbitrarily set the threshold level μ to some value, say $\mu = 1$. In principle, the noise variances σ_{ik}^2 can be derived from the integration noise variance τ_{IF} in (1). However, the variance τ_{IF} may itself not be initially known. Instead, we simply select σ_{ik}^2 to be a constant value that is relatively large to account for initial errors in the s_i^k.

Acknowledgments

This research was supported by NSF grants 1116589 and 1254204. The authors would like to thank Bruno Olshausen, Fritz Sommer, Lav Varshney, Mitya Chlovskii, Peyman Milanfar, Evan Lyall, and Eftychios Pnevmatikakis for their insights and support. This work would not have been possible without the supportive environment and wonderful discussions at the Berkeley Redwood Center for Theoretical Neuroscience – thank you.

References

[1] R. Y. Tsien, "Fluorescent probes of cell signaling," *Ann. Rev. Neurosci.*, vol. 12, no. 1, pp. 227–253, 1989.

[2] K. Ohki, S. Chung, Y. H. Ch'ng, P. Kara, and R. C. Reid, "Functional imaging with cellular resolution reveals precise micro-architecture in visual cortex," *Nature*, vol. 433, no. 7026, pp. 597–603, 2005.

[3] J. Soriano, M. R. Martínez, T. Tlusty, and E. Moses, "Development of input connections in neural cultures," *Proc. Nat. Acad. Sci.*, vol. 105, no. 37, pp. 13 758–13 763, 2008.

[4] J. T. Vogelstein, "OOPSI: A family of optimal optical spike inference algorithms for inferring neural connectivity from population calcium imaging," Ph.D. dissertation, The John Hopkins University, 2009.

[5] C. Stosiek, O. Garaschuk, K. Holthoff, and A. Konnerth, "In vivo two-photon calcium imaging of neuronal networks," *Proc. Nat. Acad. Sci.*, vol. 100, no. 12, pp. 7319–7324, 2003.

[6] K. Svoboda and R. Yasuda, "Principles of two-photon excitation microscopy and its applications to neuroscience," *Neuron*, vol. 50, no. 6, pp. 823–839, 2006.

[7] O. Yizhar, L. E. Fenno, T. J. Davidson, M. Mogri, and K. Deisseroth, "Optogenetics in neural systems," *Neuron*, vol. 71, no. 1, pp. 9–34, 2011.

[8] Y. Mishchenko, J. T. Vogelstein, and L. Paninski, "A Bayesian approach for inferring neuronal connectivity from calcium fluorescent imaging data," *Ann. Appl. Stat.*, vol. 5, no. 2B, pp. 1229–1261, Feb. 2011.

[9] O. Stetter, D. Battaglia, J. Soriano, and T. Geisel, "Model-free reconstruction of excitatory neuronal connectivity from calcium imaging signals," *PLoS Computational Biology*, vol. 8, no. 8, p. e1002653, 2012.

[10] A. Dempster, N. M. Laird, and D. B. Rubin, "Maximum-likelihood from incomplete data via the EM algorithm," *J. Roy. Statist. Soc.*, vol. 39, pp. 1–17, 1977.

[11] A. Doucet, S. Godsill, and C. Andrieu, "On sequential Monte Carlo sampling methods for Bayesian filtering," *Statistics and Computing*, vol. 10, no. 3, pp. 197–208, 2000.

[12] A. Doucet and A. M. Johansen, "A tutorial on particle filtering and smoothing: Fifteen years later," *Handbook of Nonlinear Filtering*, vol. 12, pp. 656–704, 2009.

[13] P. Dayan and L. F. Abbott, *Theoretical Neuroscience. Computational and Mathematical Modeling of Neural Systems*. MIT Press, 2001.

[14] J. T. Vogelstein, B. O. Watson, A. M. Packer, R. Yuste, B. Jedynak, and L. Paninski, "Spike inference from calcium imaging using sequential monte carlo methods," *Biophysical J.*, vol. 97, no. 2, pp. 636–655, 2009.

[15] M. J. Wainwright and M. I. Jordan, "Graphical models, exponential families, and variational inference," *Found. Trends Mach. Learn.*, vol. 1, 2008.

[16] D. L. Donoho, A. Maleki, and A. Montanari, "Message-passing algorithms for compressed sensing," *Proc. Nat. Acad. Sci.*, vol. 106, no. 45, pp. 18 914–18 919, Nov. 2009.

[17] T. P. Minka, "A family of algorithms for approximate Bayesian inference," Ph.D. dissertation, Massachusetts Institute of Technology, Cambridge, MA, 2001.

[18] A. K. Fletcher, S. Rangan, L. Varshney, and A. Bhargava, "Neural reconstruction with approximate message passing (NeuRAMP)," in *Proc. Neural Information Process. Syst.*, Granada, Spain, Dec. 2011.

[19] U. S. Kamilov, S. Rangan, A. K. Fletcher, and M. Unser, "Approximate message passing with consistent parameter estimation and applications to sparse learning," in *Proc. NIPS*, Lake Tahoe, NV, Dec. 2012.

[20] S. Rangan, A. K. Fletcher, V. K. Goyal, and P. Schniter, "Hybrid generalized approximation message passing with applications to structured sparsity," in *Proc. IEEE Int. Symp. Inform. Theory*, Cambridge, MA, Jul. 2012, pp. 1241–1245.

[21] J. T. Vogelstein, A. M. Packer, T. A. Machado, T. Sippy, B. Babadi, R. Yuste, and L. Paninski, "Fast nonnegative deconvolution for spike train inference from population calcium imaging," *J. Neurophysiology*, vol. 104, no. 6, pp. 3691–3704, 2010.

[22] J. Oñativia, S. R. Schultz, and P. L. Dragotti, "A finite rate of innovation algorithm for fast and accurate spike detection from two-photon calcium imaging," *J. Neural Engineering*, vol. 10, no. 4, p. 046017, 2013.

[23] E. A. Pnevmatikakis and L. Paninski, "Sparse nonnegative deconvolution for compressive calcium imaging: algorithms and phase transitions," in *Advances in Neural Information Processing Systems*, 2013, pp. 1250–1258.

[24] C. M. Bishop, *Pattern Recognition and Machine Learning*, ser. Information Science and Statistics. New York, NY: Springer, 2006.

[25] D. L. Donoho, "Compressed sensing," *IEEE Trans. Inform. Theory*, vol. 52, no. 4, pp. 1289–1306, Apr. 2006.

[26] A. Montanari, "Graphical model concepts in compressed sensing," in *Compressed Sensing: Theory and Applications*, Y. C. Eldar and G. Kutyniok, Eds. Cambridge Univ. Press, Jun. 2012, pp. 394–438.

[27] S. Rangan, "Generalized approximate message passing for estimation with random linear mixing," in *Proc. IEEE Int. Symp. Inform. Theory*, Saint Petersburg, Russia, Jul.–Aug. 2011, pp. 2174–2178.

[28] M. Seeger, "Bayesian inference and optimal design for the sparse linear model," *J. Machine Learning Research*, vol. 9, pp. 759–813, Sep. 2008.

[29] S. Rangan, P. Schniter, E. Riegler, A. Fletcher, and V. Cevher, "Fixed points of generalized approximate message passing with arbitrary matrices," in *Proc. ISIT*, Jul. 2013, pp. 664–668.

[30] F. Krzakala, A. Manoel, E. W. Tramel, and L. Zdeborová, "Variational free energies for compressed sensing," in *Proc. ISIT*, Jul. 2014, pp. 1499–1503.

[31] S. Rangan, P. Schniter, and A. Fletcher, "On the convergence of approximate message passing with arbitrary matrices," in *Proc. ISIT*, Jul. 2014, pp. 236–240.

[32] R. Tibshirani, "Regression shrinkage and selection via the lasso," *J. Royal Stat. Soc., Ser. B*, vol. 58, no. 1, pp. 267–288, 1996.

[33] N. Soltani and A. Goldsmith, "Directed information between connected leaky integrate-and-fire neurons," in *Proc. IEEE Int. Symp. Inform. Theory*, Honolulu, HI, Jun. 2014, pp. 1291–1295.

[34] R. Sayer, M. Friedlander, and S. Redman, "The time course and amplitude of EPSPs evoked at synapses between pairs of CA3/CA1 neurons in the hippocampal slice," *J. Neuroscience*, vol. 10, no. 3, pp. 826–836, 1990.

[35] S. Keshri, E. Pnevmatikakis, A. Pakman, B. Shababo, and L. Paninski, "A shotgun sampling solution for the common input problem in neural connectivity inference," *arXiv e-Print arXiv:1309.3724*, 2013.